



Acid-catalyzed kinetics of indium tin oxide etching



Jae-Hyeok Choi^{a,b}, Seong-Oh Kim^{a,b}, Diana L. Hilton^{a,b}, Nam-Joon Cho^{a,b,c,*}

^a School of Materials Science and Engineering, Nanyang Technological University, 50 Nanyang Avenue, 639798, Singapore

^b Centre for Biomimetic Sensor Science, Nanyang Technological University, 50 Nanyang Drive, 637553, Singapore

^c School of Chemical and Biomedical Engineering, Nanyang Technological University, 62 Nanyang Drive, 637459, Singapore

ARTICLE INFO

Article history:

Received 22 January 2014

Received in revised form 21 June 2014

Accepted 26 June 2014

Available online 5 July 2014

Keywords:

Indium tin oxide

Etching

Quartz crystal microbalance

Contact angle

X-ray photoelectron spectroscopy

Atomic force microscopy

ABSTRACT

We report the kinetic characterization of indium tin oxide (ITO) film etching by chemical treatment in acidic and basic electrolytes. It was observed that film etching increased under more acidic conditions, whereas basic conditions led to minimal etching on the time scale of the experiments. Quartz crystal microbalance was employed in order to track the reaction kinetics as a function of the concentration of hydrochloric acid and accordingly solution pH. Contact angle measurements and atomic force microscopy experiments determined that acid treatment increases surface hydrophilicity and porosity. X-ray photoelectron spectroscopy experiments identified that film etching is primarily caused by dissolution of indium species. A kinetic model was developed to explain the acid-catalyzed dissolution of ITO surfaces, and showed a logarithmic relationship between the rate of dissolution and the concentration of undissociated hydrochloric acid molecules. Taken together, the findings presented in this work verify the acid-catalyzed kinetics of ITO film dissolution by chemical treatment, and support that the corresponding chemical reactions should be accounted for in ITO film processing applications.

© 2014 Elsevier B.V. All rights reserved.

1. Introduction

Indium tin oxide (ITO) is a transparent conducting oxide [1,2] that is widely employed as a thin film coating in many types of optoelectronic devices, including liquid crystal displays [3–6] and solar panels [7]. Chemical stability of ITO films is therefore an important factor for device fabrication and processing as well as for long-term issues such as dissolution and degradation [8–11], durability [12] and corrosion [13]. ITO films may be treated by one or more types of processing steps, including chemical etching or leaching (acid or base treatment) [14–19], oxidation (oxygen plasma) [20–23] and annealing [2,24]. In addition to their possible coating applications, ITO films can also serve as a substrate for deposition of electroactive materials, including metal oxides, ceramics and conducting polymers. The deposition process typically involves cathodic polarization in aqueous electrolytes [25–28]. As device fabrication and processing can be performed in a variety of electrochemical and electrolyte conditions, there has been significant interest in correlating fabrication and processing methods with resulting structural, optical and electrical properties of the ITO film.

Early speculation predicted that structural changes in ITO films may arise under negative applied potentials, and Armstrong et al. [29] provided the first direct evidence to show that changes in the chemical composition of an ITO film surface can occur as a function of electrolysis potential. Film instability under anodic potential cycling has also been

observed [30], and it is now understood that both cathodic and anodic potentials can affect ITO film properties [27,28,31,32]. While high applied potentials and corresponding electrochemical reactions are one contributing factor to induce changes in ITO film properties, chemical reactions that involve the breaking of surface bonds may also occur [33,34]. Indeed, ITO film processing and electrochemical deposition is generally performed in acidic or alkaline conditions, with a preference toward concentrated acids [19,25–28,35,36]. Furthermore, ITO films exhibit higher corrosion rates in acidic solutions, as compared to neutral solutions, suggesting that the aqueous electrolyte contains chemically active species.

Based on high corrosion rates observed in acidic solutions, it would appear that acidic conditions promote chemical reactions on the ITO surface. Adding to the complexity, there can be significant variation in the reaction kinetics depending on the type of acid [33,36]. A range of acids have been tested for ITO film etching and halogen acids are the most active and therefore widely used for film processing [33]. As a representative halogen acid, hydrochloric acid solutions etch ITO films via a non-electrochemical mechanism and the etch rate depends on the concentration of undissociated hydrochloric acid molecule, which is the active species. Weak acids such as acrylic acid have also been identified to affect electrochemical and structural properties of ITO films [36]. However, a large fraction of studies have been oriented toward electrochemical deposition and have therefore simultaneously examined the effects of the aqueous electrolyte and applied potential on ITO surface characteristics. Although this approach has led to practical insights for device fabrication and processing, it also raises a fundamental question about the role of electrochemical versus non-

* Corresponding author at: School of Materials Science and Engineering, Nanyang Technological University, 50 Nanyang Avenue, 639798, Singapore.

E-mail address: njcho@ntu.edu.sg (N.-J. Cho).

electrochemical reactions occurring on the ITO surface and its corresponding effects on film properties, including structural morphology. Recently, Spada et al. [32] reported that electrochemical effects on ITO film properties can occur in a manner that is largely independent of solution pH. In relation to previous works on the subject, their findings support that the effect of solution pH on ITO film properties (e.g., morphology, structure, chemical composition) remains to be elucidated further, especially in terms of chemical reaction kinetics.

However, it is challenging to study the reaction kinetics occurring on ITO film surfaces because most chemical, colorimetric and spectroscopic methods do not track the reaction progress. As a result, most studies have analyzed the surface properties of an ITO film after treatment under the desired conditions. One promising technique to study reaction kinetics is the quartz crystal microbalance (QCM), which is able to monitor changes in the adsorbed mass of the ITO film. Using the QCM technique, Folcher et al. [35] identified that the rate of ITO film corrosion (i.e., monitored as dissolution) under a cathodic potential increases appreciably in solutions with high concentrations of hydrochloric acid, as compared to solutions with lower concentrations. As these experiments were performed under a cathodic potential, ITO film dissolution was likely due to a combination of electrochemical and chemical reactions. A systematic investigation of how the chemical environment influences ITO film dissolution in the absence of an applied potential has not been reported yet. In this work, we investigate the kinetics of ITO film etching by chemical processes in acidic and basic electrolytes. ITO film dissolution was tracked by the QCM measurement technique along with secondary characterization by contact angle measurement, atomic force microscopy (AFM) and X-ray photoelectron spectroscopy (XPS).

2. Experimental details

2.1. Sample preparation

Experiments were performed on ITO-coated (Q5X999) QCM sensor chips (Q-Sense AB, Göthenburg, Sweden). The ITO thin films (~150 nm thickness) were sputter-coated on top of a Quartz–Cr–Au–Ti-based adhesive layer. The ITO substrates were cleaned with 1% sodium dodecyl sulfate (99%, Alfa Aesar) solution, and then rinsed with deionized water and finally ethanol in sequential order. Immediately before experiment, the substrates were dried with a gentle stream of nitrogen air and treated with oxygen plasma (Harrick Plasma, Ithaca, NY, USA) for 1 min. For all experiments, a 10 mM Tris buffer solution [pH 7.5] with 150 mM NaCl was freshly prepared and the solution pH was adjusted by 1 M hydrochloric acid (Merck Millipore) or 1 M sodium hydroxide (BioXtra, Sigma-Aldrich). Stock buffer solutions were prepared from pH 2 to pH 12, and the pH values were checked before use. All buffer solutions were prepared with deionized water (resistivity of >18 M Ω ·cm, Millipore, Oregon, USA).

2.2. Quartz crystal microbalance (QCM)

The Q-Sense E4 instrument (Q-Sense) was used for QCM experiments. The QCM technique measures the change in the resonance frequency, Δf , and energy dissipation, ΔD , when a material either adsorbs onto or desorbs from the surface of an oscillating, AT-cut piezoelectric crystal quartz crystal with a fundamental frequency of 5 MHz. QCM measurements were recorded at the fundamental frequency and selected overtones ($n = 3$ –9).

2.3. X-ray photoelectron spectroscopy (XPS)

XPS measurements were conducted on a Kratos XPS system with a monochromated Al–K alpha source for high resolution, ~0.3 eV. Measurements were performed on ITO-coated surfaces after QCM experiment. Measurements were recorded under ultra-high vacuum

(UHV) at a pressure of 5×10^{-9} Torr. The take-off angle was 90°. Atomic concentration percentage calculations and peak analysis were performed with the CasaXPS software and OriginPro 8.5. The XPS measurements were repeated twice. For experimental analysis, the first C1s peak (peak 1) was shifted from ~285.5 eV to ~284.3 eV [37]. Accordingly, all XPS data was shifted and compared to the main reference and libraries in the Kratos XPS system [37].

2.4. Contact angle measurement

The contact angle of ITO substrates was measured with the Attension Theta Optical Tensiometer (Biolin Scientific, Stockholm, Sweden). Measurements were performed on ITO-coated surfaces after QCM experiment. Contact angle measurements were repeated at least three times for each sample. Due to the size of the QCM substrate, only static angle measurements were performed.

2.5. Atomic force microscopy (AFM)

An atomic force microscope (NX-Bio, Park Systems, South Korea) combined with an optical microscope (Eclipse Ti, Nikon, Japan) was used. A silicon nitride DNP-S10 (Veeco, USA) tip was prepared, which has a triangular shape, 18 kHz resonant frequency, and 0.06 N/m spring constant. Before experiment, the tip was treated with oxygen plasma for 5 min, and then rinsed with ethanol, water, and ethanol in sequential order before drying with a gentle stream of nitrogen air. All experiments were performed at a constant temperature of 25 °C.

3. Results and discussion

QCM experiments were conducted in order to measure ITO film stability in different pH conditions (Fig. 1). To set the measurement baseline, an ITO-coated QCM crystal was first incubated in 10 mM Tris buffer solution [pH 7.5] with 150 mM NaCl. Two sets of independent experiments were then performed, acidic and basic titrations. In the basic titration series, the bulk solution in the QCM measurement chamber was exchanged incrementally with increasingly basic buffer solutions. The new buffer was introduced under flow conditions for 5 min, and then the flow was stopped and the incubation proceeded under equilibrium conditions. The titration range was pH 7.5 to 12.0, and the titration increment was 0.5 pH units upward. Across the range, there was a change in frequency of less than 5 Hz and no change in energy dissipation (Fig. 1A). Using the Sauerbrey relationship which converts the change in frequency to the change in adsorbed mass for non-viscoelastic films, the QCM frequency shift corresponds to mass desorption of 40 ng·cm⁻² from the ITO surface (Fig. 1B).

In the acidic titration series, a similar protocol was used in the pH range 7.5 to 2.5 downward. In contrast to the basic titration series, acidic titration caused an appreciably larger change in frequency of more than 450 Hz (Fig. 1C). However, again, there was no change in energy dissipation. The QCM frequency shift corresponds to mass desorption of more than 7900 ng·cm⁻², as determined by the Sauerbrey relationship (Fig. 1D). The desorption behavior indicates that acidic conditions promote significant ITO film degradation. In addition to general trends across the pH range, the acidic titration series shows that the rate of mass desorption became greater with increasingly acidic pH conditions. Within each titration step, an equilibrium in the frequency shift was reached during the QCM measurement, as discussed further below.

After the QCM experiments were finished, additional surface characterization experiments were performed. Base- and acid-treated samples refer to the ITO surfaces which were subjected to the basic or acidic titration series, respectively. Contact angle measurements were performed in order to measure surface hydrophilicity (Fig. 2). The contact angle of a control ITO-coated QCM crystal incubated only in 10 mM Tris buffer solution [pH 7.5] with 150 mM NaCl (without titration) was 61.9° ± 8.4°. In contrast, the contact angle of the base-treated ITO

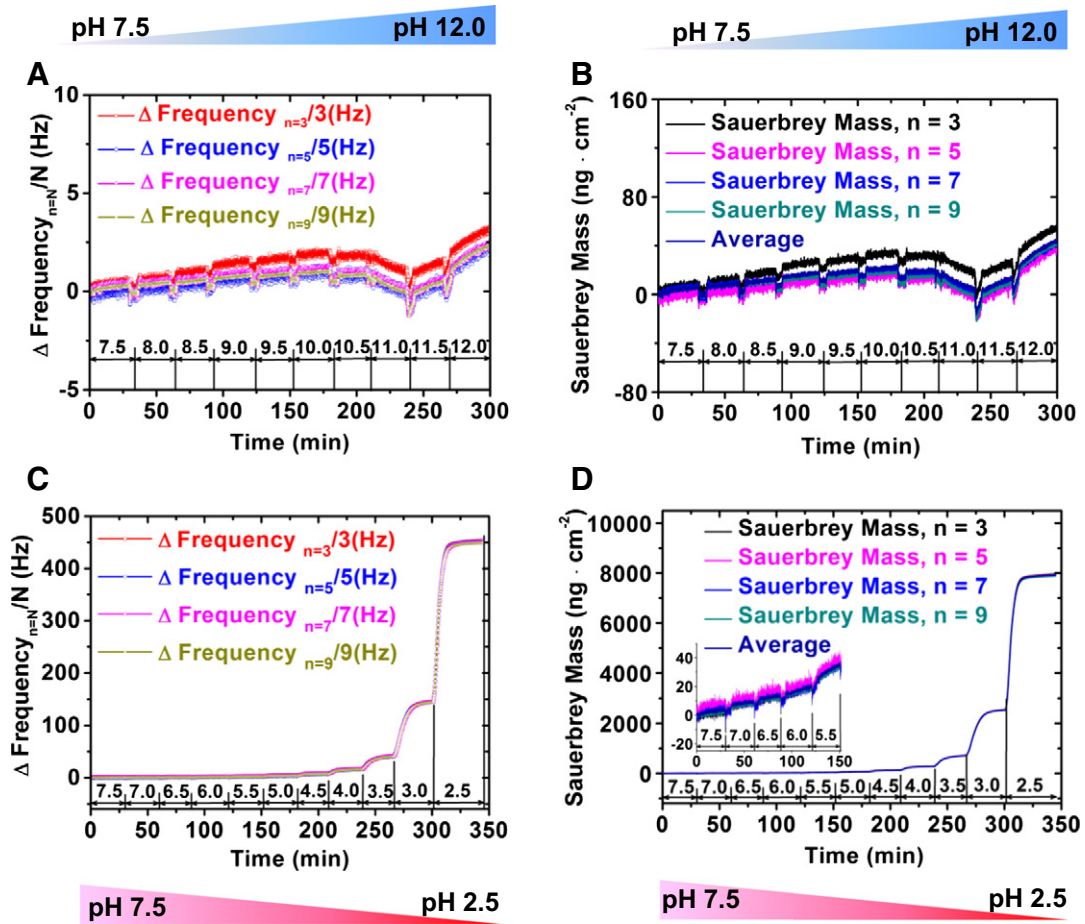


Fig. 1. QCM monitoring of ITO surfaces incubated in acidic or basic electrolytes. QCM measurements were performed to track adsorption/desorption processes occurring on an ITO-coated surface as increasingly acidic or basic solutions were introduced into the measurement chamber. The shift in QCM frequency as a function of time is presented for the (A) basic and (C) acidic titration series. The corresponding changes in Sauerbrey mass as a function of time are presented for the (B) basic and (D) acidic titration series.

surface was $33.9^\circ \pm 9.4^\circ$. As there was only minor desorption observed in the corresponding QCM measurement, the change in hydrophilicity is likely due to changes in the ITO surface chemistry. The isoelectric point (IEP) of ITO surfaces is around 6 [38]. With increasing pH above the IEP, the surface becomes increasingly negatively charged which is consistent with deprotonation of oxide groups on the film surface. The contact angle of the acid-treated ITO was $29.7^\circ \pm 6.5^\circ$. Based on the QCM measurement data indicating mass desorption, the increase in hydrophilicity in acidic conditions is probably due to mass desorption, i.e., increased film porosity.

To investigate morphological effects of the acidic and basic titration series on ITO surface characteristics, the ITO-coated QCM

crystals were also characterized by atomic force microscopy (Fig. 3). The control surface had a homogenous film surface, with consistent-size ITO grains (diameter between 50 and 80 nm) and an average surface roughness of 0.596 nm. By contrast, the ITO surfaces treated in acidic or basic conditions had appreciably coarser features. The base-treated ITO surface had an average surface roughness of 1.554 nm and more discernible surface features, including a granular appearance. This effect is likely due to ITO dissolution which occurs preferably at the grain boundaries. Even more so, the acid-treated ITO surface had an average surface roughness of 2.709 nm and significantly greater surface dissolution. The formation of spherical particles on the ITO surface was due to dissolution at the

	Control	Base-Treated	Acid-Treated
Contact Angle (°)	61.9 ± 8.4	33.9 ± 9.4	29.7 ± 6.5
Static Angle Image Recording			

Fig. 2. Contact angle measurement on treated ITO surfaces. Contact angle experiments in static angle mode were performed on ITO-coated surfaces after the QCM experiments were completed. The control sample was an ITO-coated surface incubated only in 10 mM Tris buffer solution [pH 7.5] with 150 mM NaCl.

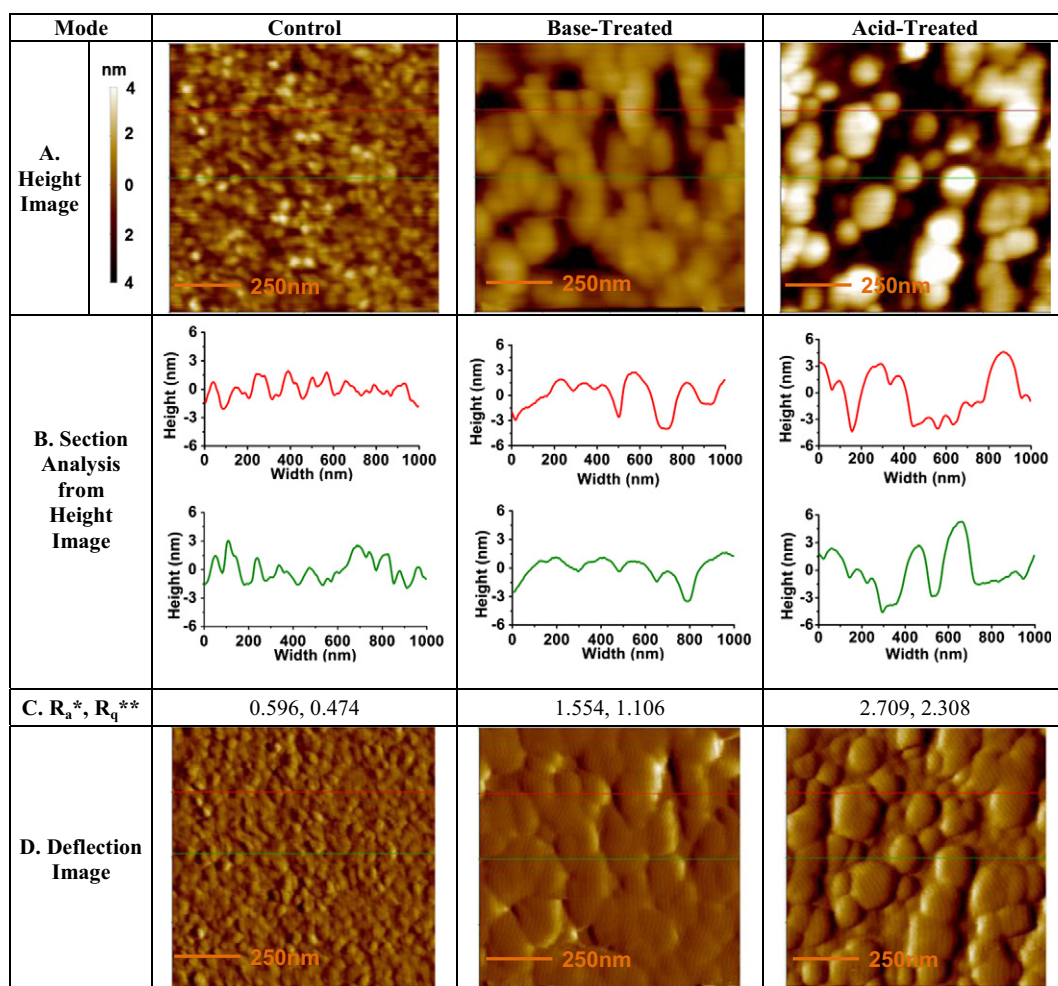


Fig. 3. Atomic force microscopy imaging of treated ITO surfaces. AFM experiments were performed on ITO-coated surfaces after the QCM experiments were completed. (A) Height mode images, (B) section analysis, (C) roughness average and root mean square roughness, and (D) deflection mode images, are presented for control, base-treated, and acid-treated samples, respectively. The control sample was an ITO-coated surface incubated only in 10 mM Tris buffer solution [pH 7.5] with 150 mM NaCl. *Roughness average. **Root mean square roughness.

grain boundaries, and has been previously reported by Huang et al. [19] for an electrochemical reaction on the ITO surface also involving hydrochloric acid. The findings herein support that a chemical reaction under appropriate conditions can have similar effects on ITO surface morphology as electrochemical reactions. Taken together,

the AFM experiments provide direct evidence that chemical processes can cause ITO film degradation via dissolution at grain boundaries.

ITO film surfaces have a variety of chemical species so X-ray photoelectron spectroscopy (XPS) experiments were next performed to identify if there was selective disassociation of one or more species (Fig 4).

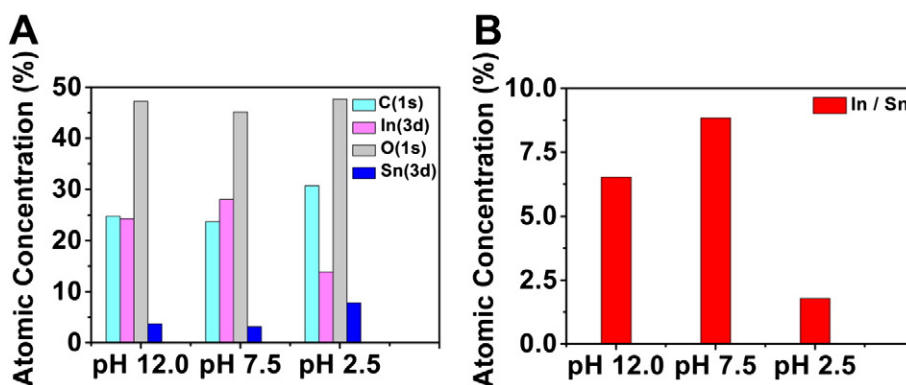


Fig. 4. X-ray photoelectron spectroscopy analysis of ITO surface composition. XPS experiments were performed on ITO-coated surfaces after the QCM experiments were completed. The data presented is as follows: (A) atomic concentration percentage of C(1s), In(3d), O(1s), and Sn(3d), (B) In/Sn ratio. The control sample was an ITO-coated surface incubated only in 10 mM Tris buffer solution [pH 7.5] with 150 mM NaCl.

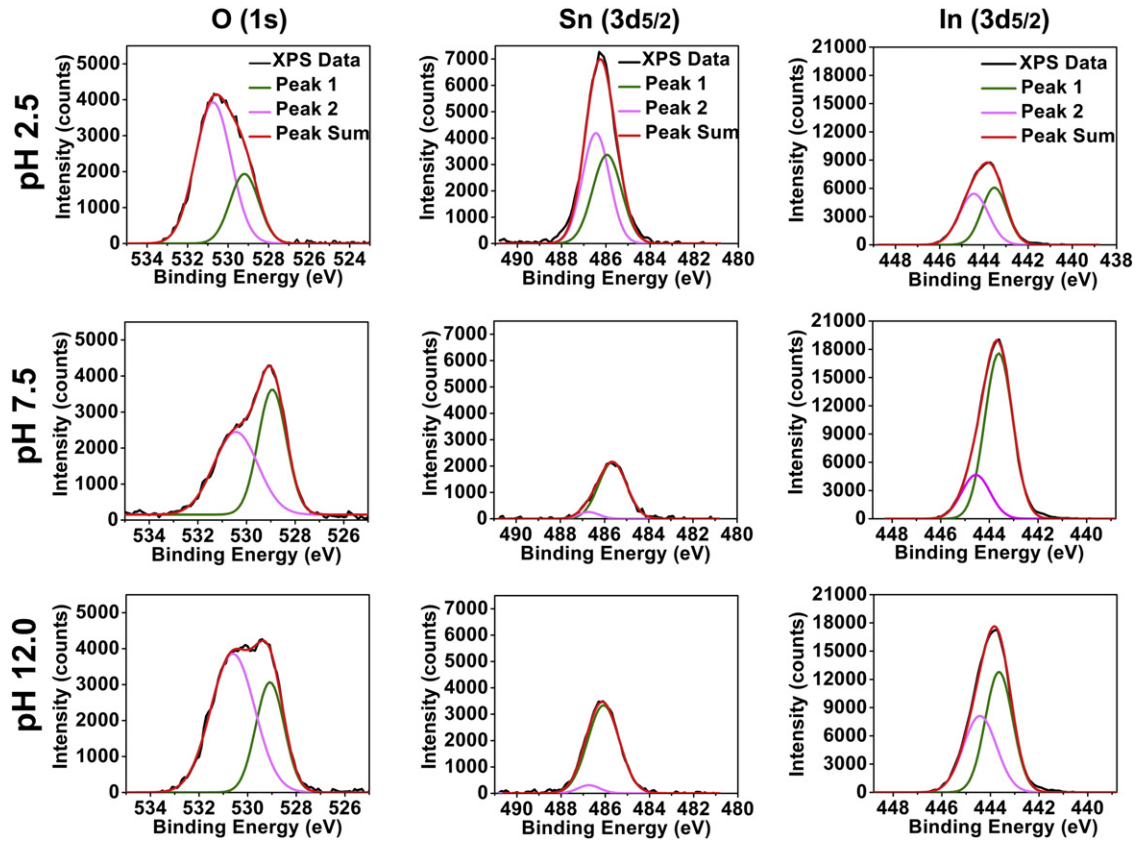


Fig. 5. XPS spectra and peak analysis. (A) O(1s) peaks, (B) Sn(3d_{5/2}) peaks, and (C) In(3d_{5/2}) peaks are presented.

Compared to the control ITO surface, there was a small decrease in the atomic concentration of In(3d) on the base-treated ITO surface and a more appreciable decrease on the acid-treated ITO surface (Fig. 4A). Accordingly, the In/Sn atomic ratio for the control and base-treated samples (8.84 and 6.52, respectively) were appreciably larger than for the acid-treated sample (1.78) (Fig. 4B). The XPS experimental results clearly identify that acidic conditions promote indium dissolution. Previous work by Huang et al. [19] demonstrated that indium dissolution increases surface roughness and porosity, especially near the grain boundaries. Collectively, the XPS and AFM experiments therefore support that acidic treatment of the ITO surface causes indium dissolution and accordingly film porosity increases.

Spectral decomposition of certain atomic peaks was also performed in order to estimate which indium species were disassociated (Fig. 5). Compared to the control sample, the acid-treated sample had a decrease in In₂O₃ and an increase in reaction products, indium hydroxide and oxy-hydroxide, due to incomplete hydrolysis. The findings provide evidence to propose a mechanism to explain indium dissolution. Chemically, acidity in our system is related to the molar concentration of hydrochloric acid. Consistent with previous works [33,34] on halogen acid treatment of ITO surfaces, we therefore assume that the undissociated hydrochloric acid molecule is the active species that catalyzes indium dissolution. One reaction product would be indium chloride (InCl₃), which is ionized and dissolved in the solution. However, the acid-treated ITO sample would have more indium hydroxides at the grain boundaries because this product has poor solubility in aqueous solution [37].

To clarify the mechanism of ITO film dissolution by hydrochloric acid, a kinetic model was developed. Within each titration step, there were three kinetic regimes: Stage A represents the mixing period during solution exchange. This stage showed nonlinear reaction kinetics and was not included in the kinetic modeling; Stage B represents the linear

reaction kinetics when there was saturation of reactants; and Stage C is the nonlinear region when there is no longer saturation of reactants (Fig. 6). In Stage B, the reaction progress can be represented as [39]

$$\frac{dm_{net}}{dt} = k_{net} \left(1 - e^{\Delta G_R/RT}\right) \quad (1)$$

where $\frac{dm_{net}}{dt}$ is the net reaction rate, k_{net} is the dissolution rate, and ΔG_R is the Gibbs free energy of the reaction. As the dissolution reaction is in non-equilibrium conditions in Stage B, $\Delta G_R \ll 0$ so $e^{\Delta G_R/RT}$ will approach zero. Accordingly, the dissolution rate can be simplified as follows

$$\frac{dm_{net}}{dt} = k_{net}. \quad (2)$$

Using Eq. (2), the QCM frequency shifts were fit to the linear model, $k_{net}a + b$, where a and b are fitting parameters. As presented in Table 1, k_{net} varied from $3.16 \pm 0.05 \text{ ng} \cdot \text{cm}^{-2} \cdot \text{min}^{-1}$ at pH 5.0 to $782.04 \pm 2.79 \text{ ng} \cdot \text{cm}^{-2} \cdot \text{min}^{-1}$ at pH 2.5. The net dissolution rate was strongly affected by solution pH and accordingly the molar concentration of hydrochloric acid molecules in solution (Table 1). Importantly, the logarithm of the reaction rate had a linear dependence on the solution pH (Fig. 7). The model results support that, in the absence of an applied potential, hydrochloric acid may catalyze ITO film dissolution via a strictly chemical reaction. A schematic describing the reaction steps associated with acid-catalyzed dissolution of ITO thin films is presented in Fig. 8. Based on these findings, it is evident that solution pH influences ITO film dissolution and hence appropriate solution conditions should be chosen to achieve a balance between electrochemical and non-electrochemical reactions occurring on ITO surfaces.

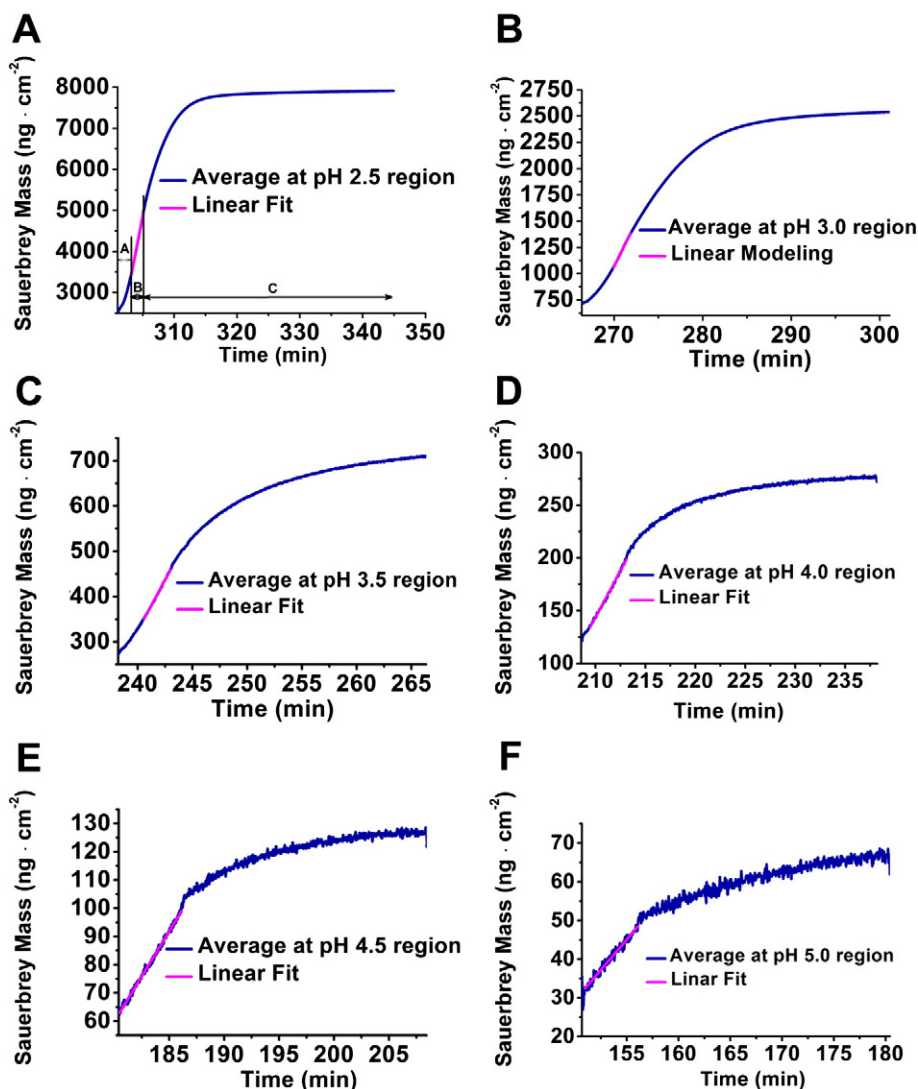


Fig. 6. Kinetic analysis of ITO surface dissolution by hydrochloric acid. Sauerbrey model analysis for region B by linear fit in the following conditions: (A) pH 2.5, (B) pH 3.0, (C) pH 3.5, (D) pH 4.0, (E) pH 4.5, and (F) pH 5.0.

4. Conclusions

ITO films are susceptible to degradation by a variety of electrochemical and chemical reactions. Clarifying the relative role of electrochemical versus chemical reactions in ITO film dissolution is desirable. In this work, QCM measurements supported that ITO film etching increases under more acidic conditions. This finding was corroborated by contact angle, AFM and XPS measurements. Building on previous works [35,40] which investigated how hydrochloric acid influences ITO film dissolution, the experiments presented herein were performed under well-controlled conditions, i.e., the acidic titration series was performed

from pH 7.5 to pH 2.5 in 0.5 pH unit increments. A kinetic model was applied to explain the acid-catalyzed dissolution of ITO surfaces. The key finding was that, in the acidic titration series, the logarithm of the

Table 1

QCM dissolution kinetics of acid-treated ITO surface. Based on the Sauerbrey mass corresponding to mass dissolution, k_{net} was calculated as a function of solution pH.

pH	k_{net} (ng · cm ⁻² · min ⁻¹)
2.5	782.04 ± 2.79
3.0	170.15 ± 0.61
3.5	44.70 ± 0.19
4.0	17.60 ± 0.11
4.5	6.38 ± 0.04
5.0	3.16 ± 0.05

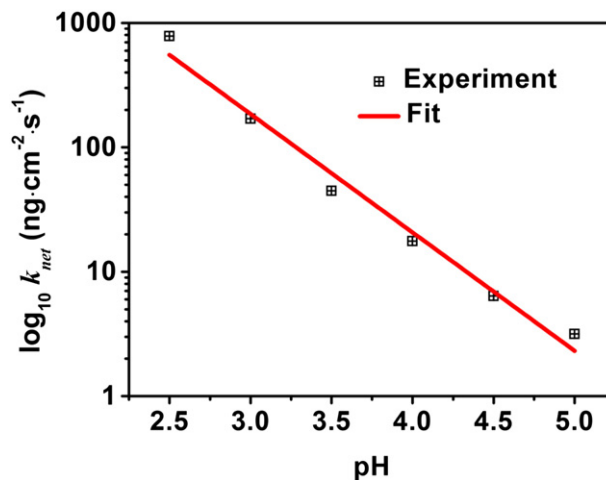


Fig. 7. Acid-catalyzed dissolution of ITO surface. In the acidic titration series, there was a linear trend between the logarithm of k_{net} and the solution pH.

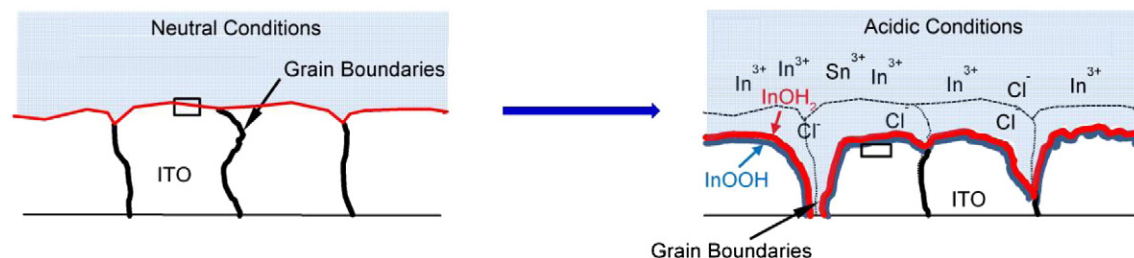


Fig. 8. Schematic of acid-catalyzed dissolution of ITO surface. Under acidic conditions, chemical dissolution of ITO thin films occurs at the grain boundaries. The rectangular boxes indicate the representative areas where ITO interacts with solution.

reaction rate depended linearly on the solution pH. This finding verifies that hydrochloric acid catalyzes ITO film dissolution via a chemical process, and underscores that the corresponding chemical reactions should be accounted for in order to optimize ITO film processing.

Acknowledgments

The authors wish to acknowledge support from the National Research Foundation (NRF – NRF2011-01) and Nanyang Technological University to N.J.C.

References

- [1] C.W. Tang, S.A. Vanslyke, Organic electroluminescent diodes, *Appl. Phys. Lett.* 51/12 (1987) 913.
- [2] H. Kim, C.M. Gilmore, A. Pique, J.S. Horwitz, H. Mattoussi, H. Murata, Z.H. Kafafi, D.B. Chrisey, Electrical, optical, and structural properties of indium–tin-oxide thin films for organic light-emitting devices, *J. Appl. Phys.* 86/11 (1999) 6451.
- [3] Y.Y. Kee, S.S. Tan, T.K. Yong, C.H. Nee, S.S. Yap, T.Y. Tou, G. Safran, Z.E. Horvath, J.P. Moscatello, Y.K. Yap, Low-temperature synthesis of indium tin oxide nanowires as the transparent electrodes for organic light emitting devices, *Nanotechnology* 23 (2) (2012).
- [4] M. Katayama, TFT-LCD technology, *Thin Solid Films* 341/1-2 (1999) 140.
- [5] H. Kobayashi, T. Ishida, Y. Nakato, H. Tsubomura, Mechanism of carrier transport in highly efficient solar-cells having indium tin oxide Si junctions, *J. Appl. Phys.* 69/3 (1991) 1736.
- [6] C. Cotal, A. Azema, J.C. Roustan, Fabrication and characterization of ITO thin films deposited by excimer laser evaporation, *Thin Solid Films* 288/1-2 (1996) 248.
- [7] A.C. Arango, D.C. Oertel, Y.F. Xu, M.G. Bawendi, V. Bulovic, Heterojunction photovoltaics using printed colloidal quantum dots as a photosensitive layer, *Nano Lett.* 9/2 (2009) 860.
- [8] H. Aziz, G. Xu, A degradation mechanism of organic light-emitting devices, *Synth. Met.* 80/1 (1996) 7.
- [9] M.P. de Jong, L.J. van Ijzendoorn, M.J.A. de Voigt, Stability of the interface between indium–tin-oxide and poly(3,4-ethylenedioxythiophene)/poly(styrenesulfonate) in polymer light-emitting diodes, *Appl. Phys. Lett.* 77/14 (2000) 2255.
- [10] F.C. Krebs, K. Norrman, Analysis of the failure mechanism for a stable organic photovoltaic during 10,000 h of testing, *Prog. Photovoltaics* 15/8 (2007) 697.
- [11] M. Jorgensen, K. Norrman, F.C. Krebs, Stability/degradation of polymer solar cells, *Sol. Energy Mater. Sol. Cells* 92/7 (2008) 686.
- [12] O.M.R. Chyan, K. Rajeshwar, Heterojunction photoelectrodes. 2. Electrochemistry at tin-doped indium oxide aqueous-electrolyte interfaces, *J. Electrochem. Soc.* 132/9 (1985) 2109.
- [13] J.E.A.M. Vandenmeerakker, W.R. Terveen, Reductive corrosion of ITO in contact with Al in alkaline-solutions, *J. Electrochem. Soc.* 139/2 (1992) 385.
- [14] C.H. Huang, H.Y. Chou, C.W. Lian, T.Y. Tseng, Electrical and dielectric behavior of fluorite-like $\text{Sr}_{0.8}\text{Bi}_{0.2}\text{Ta}_2\text{O}_9$ thin films pyrolyzed and thermally annealed at 450 degrees C, *Mater. Chem. Phys.* 83/2-3 (2004) 345.
- [15] F. Nuesch, E.W. Forsythe, Q.T. Le, Y. Gao, L.J. Rothberg, Importance of indium tin oxide surface acid basicity for charge injection into organic materials based light emitting diodes, *J. Appl. Phys.* 87/11 (2000) 7973.
- [16] F. Nuesch, K. Kamaras, L. Zuppiroli, Protonated metal-oxide electrodes for organic light emitting diodes, *Chem. Phys. Lett.* 283/3-4 (1998) 194.
- [17] F. Nuesch, Y. Li, L.J. Rothberg, Patterned surface dipole layers for high-contrast electroluminescent displays, *Appl. Phys. Lett.* 75/12 (1999) 1799.
- [18] Q.T. Le, F. Nuesch, L.J. Rothberg, E.W. Forsythe, Y.L. Gao, Photoemission study of the interface between phenyl diamine and treated indium–tin-oxide, *Appl. Phys. Lett.* 75/10 (1999) 1357.
- [19] C.A. Huang, K.C. Li, G.C. Tu, W.S. Wang, The electrochemical behavior of tin-doped indium oxide during reduction in 0.3 M hydrochloric acid, *Electrochim. Acta* 48/24 (2003) 3599.
- [20] J.S. Kim, M. Granstrom, R.H. Friend, N. Johansson, W.R. Salaneck, R. Daik, W.J. Feast, F. Cacialli, Indium–tin oxide treatments for single- and double-layer polymeric light-emitting diodes: the relation between the anode physical, chemical, and morphological properties and the device performance, *J. Appl. Phys.* 84/12 (1998) 6859.
- [21] J.S. Kim, P.K.H. Ho, D.S. Thomas, R.H. Friend, F. Cacialli, G.W. Bao, S.F.Y. Li, X-ray photoelectron spectroscopy of surface-treated indium–tin oxide thin films, *Chem. Phys. Lett.* 315/5-6 (1999) 307.
- [22] J.S. Kim, R.H. Friend, F. Cacialli, Surface energy and polarity of treated indium–tin-oxide anodes for polymer light-emitting diodes studied by contact-angle measurements, *J. Appl. Phys.* 86/5 (1999) 2774.
- [23] J.S. Kim, R.H. Friend, F. Cacialli, Improved operational stability of polyfluorene-based organic light-emitting diodes with plasma-treated indium–tin-oxide anodes, *Appl. Phys. Lett.* 74/21 (1999) 3084.
- [24] U. Betz, M.K. Olsson, J. Marthy, M.F. Escola, F. Atamny, Thin films engineering of indium tin oxide: large area flat panel displays application, *Surf. Coat. Technol.* 200/20-21 (2006) 5751.
- [25] W.J. Gao, S. Cao, Y.Z. Yang, H. Wang, J. Li, Y.M. Jiang, Electrochemical impedance spectroscopy investigation on indium tin oxide films under cathodic polarization in NaOH solution, *Thin Solid Films* 520/23 (2012) 6916.
- [26] E. Matveeva, Electrochemistry of the indium–tin oxide electrode in 1 M NaOH electrolyte, *J. Electrochem. Soc.* 152/9 (2005) H138.
- [27] M. Senthilkumar, J. Mathiyarasu, J. Joseph, K.L.N. Phani, V. Yegnaraman, Electrochemical instability of indium tin oxide (ITO) glass in acidic pH range during cathodic polarization, *Mater. Chem. Phys.* 108/2-3 (2008) 403.
- [28] J. Stotter, Y. Show, S.H. Wang, G. Swain, Comparison of the electrical, optical, and electrochemical properties of diamond and indium tin oxide thin-film electrodes, *Chem. Mater.* 17/19 (2005) 4880.
- [29] N.R. Armstrong, A.W. Lin, M. Fujihira, T. Kuwana, Electrochemical and surface characteristics of tin oxide and indium oxide electrodes, *Anal. Chem.* 48/4 (1976) 741.
- [30] A. Kraft, H. Hennig, A. Herbst, K.-H. Heckner, Changes in electrochemical and photoelectrochemical properties of tin-doped indium oxide layers after strong anodic polarization, *J. Electroanal. Chem.* 365/1 (1994) 191.
- [31] P.M. Bressers, E.A. Meulenkaamp, The electrochromic behavior of indium tin oxide in propylene carbonate solutions, *J. Electrochem. Soc.* 145/7 (1998) 2225.
- [32] E. Spada, F. de Paula, C. Plá Cid, G. Candiotto, R. Faria, M. Sartorelli, Role of acidic and basic electrolytes on the structure and morphology of cathodically reduced indium tin oxide (ITO) substrates, *Electrochim. Acta* 108 (2013) 520.
- [33] M. Scholten, J. Van Den Meerakker, On the mechanism of ITO etching: the specificity of halogen acids, *J. Electrochem. Soc.* 140/2 (1993) 471.
- [34] J. Van Den Meerakker, P. Baarslag, M. Scholten, On the mechanism of ITO etching in halogen acids: the influence of oxidizing agents, *J. Electrochem. Soc.* 142/7 (1995) 2321.
- [35] G. Folcher, H. Cachet, M. Froment, J. Bruneaux, Anodic corrosion of indium tin oxide films induced by the electrochemical oxidation of chlorides, *Thin Solid Films* 301/1-2 (1997) 242.
- [36] T.S. Bejital, K. Ramji, A.J. Kessman, K.A. Sierros, D.R. Cairns, Corrosion of an amorphous indium tin oxide film on polyethylene terephthalate at low concentrations of acrylic acid, *Mater. Chem. Phys.* 132/2-3 (2012) 395.
- [37] C. Donley, D. Dunphy, D. Paine, C. Carter, K. Nebesny, P. Lee, D. Alloway, N.R. Armstrong, Characterization of indium–tin oxide interfaces using X-ray photoelectron spectroscopy and redox processes of a chemisorbed probe molecule: effect of surface pretreatment conditions, *Langmuir* 18/2 (2002) 450.
- [38] J. Sun, B.V. Velamakanni, W.W. Gerberich, L.F. Francis, Aqueous latex/ceramic nanoparticle dispersions: colloidal stability and coating properties, *J. Colloid Interface Sci.* 280/2 (2004) 387.
- [39] S.A. Carrollwebb, J.V. Walther, A surface complex-reaction model for the pH-dependence of corundum and kaolinite dissolution rates, *Geochim. Cosmochim. Acta* 52/11 (1988) 2609.
- [40] C.J. Huang, Y.K. Su, S.L. Wu, The effect of solvent on the etching of ITO electrode, *Mater. Chem. Phys.* 84/1 (2004) 146.